NASA TECHNICAL MEMORANDUM

NASA TM X-1497

NASA TM X-1497

EXPERIMENTAL DETERMINATION OF NEUTRON FLUXES IN PLUM BROOK REACTOR HB-6 FACILITY WITH USE OF SULFUR PELLETS AND GOLD FOILS

by John M. Bozek and Michael P. Godlewski

Lewis Research Center
Cleveland, Ohio

NATIONAL AERONAUTICS AND SPACE ADMINISTRATION • WASHINGTON, D. C. • FEBRUARY 1968

NASA TM X-1497

EXPERIMENTAL DETERMINATION OF NEUTRON FLUXES IN PLUM BROOK REACTOR HB-6 FACILITY WITH USE OF SULFUR PELLETS AND GOLD FOILS

By John M. Bozek and Michael P. Godlewski

Lewis Research Center
Cleveland, Ohio

NATIONAL AERONAUTICS AND SPACE ADMINISTRATION

For sale by the Clearinghouse for Federal Scientific and Technical Information
Springfield, Virginia 22151 – CFSTI price $3.00

EXPERIMENTAL DETERMINATION OF NEUTRON FLUXES IN PLUM BROOK REACTOR HB-6 FACILITY WITH USE OF SULFUR PELLETS AND GOLD FOILS

by John M. Bozek and Michael P. Godlewski

Lewis Research Center

SUMMARY

Fast and thermal neutron fluxes were measured in the test cavity outside the HB-6 beam port in the Plum Brook reactor, with the use of sulfur pellets and gold foils. The dependence of flux on reactor power level, shim-control-rod position, water attenuator tank configuration, position in the test cavity, and perturbations by other experiments was investigated. Based on the measurements taken, the thermal- and fast-neutron fluxes for any combination of these parameters can be determined. Standard fluxes (which correspond approximately to an average flux in the test cavity at full reactor power) were 1.4×10^{6} neutrons per second per square centimeter (nv) for thermal neutrons ($E \leq 0.4$ eV or 0.64×10^{-7} pJ) and 8.2×10^{6} neutrons per second per square centimeter (nv) for fast neutrons ($E \geq 2.48$ MeV or 0.396 pJ). The flux errors are estimated at ±38 and ±35 percent for thermal and fast neutrons, respectively.

INTRODUCTION

Semiconductor components intended for use in nuclear space power systems must be capable of operating reliably in a nuclear environment. A radiation-effects facility was constructed (ref. 1) around the HB-6 beam hole of the NASA Plum Brook reactor facility to implement a semiconductor-device radiation study program.

A knowledge of the test-facility neutron fluxes must be available in order to assess properly radiation damage to the semiconductor devices. These fluxes were expected to change with reactor operating conditions, such as power level and shim-control-rod position, with the location of other in-core experiments, with the vertical and horizontal positions in the beam hole, and with the quantity of water in the attenuation tanks. This

report was written to provide the means to predict the fluxes as these conditions change.

Sulfur pellets and gold foils were used for the measurements described herein because their high sensitivity is desirable in the relatively low fluxes present in the HB-6 beam port. Also, the use of sulfur-pellet and gold-foil activation for neutron flux measurements is a well-established technique.

The following subjects are discussed in this report:

(1) The measurement of the activation of the pellets and foils caused by neutron fluxes at a variety of conditions (see EXPERIMENTAL DESIGN AND PROCEDURE)

(2) The analysis of the activation data which yielded the empirical prediction equation in the form of a standardized flux and six correction factors (see sections on analysis of data)

(3) The independent verification of the prediction formula and a discussion of activation analysis on sulfur pellets and gold foils

EXPERIMENTAL DESIGN AND PROCEDURE

The neutron environment in the HB-6 facility (fig. 1) of the Plum Brook reactor varies considerably with changes in the reactor parameters and the test configuration. The parameters that influence the neutron environment include shim-control-rod position, reactor power, position in the HB-6 facility, thickness of water in the attenuation tanks, and the effects of other experiments in the reactor. It is assumed that each one of the preceding parameters which influence the neutron environment in the HB-6 facility acts independently of the others. With this assumption and given information on the status of the various parameters mentioned, an empirical equation can be formulated which makes it possible to predict the neutron flux; this equation is as follows:

$$\varphi = \varphi_o \times M_1 \times M_2 \times M_3 \times M_4 \times M_5 \times M_6 \tag{1}$$

where

φ_o fast- or thermal-neutron flux for fiducial test conditions as follows:

(1) center of foil plate

(2) shim-control-rod position of 23 inches (58.5 cm)

(3) no water in attenuation tanks

(4) reactor power of 60 MW

(5) no other experiments in reactor

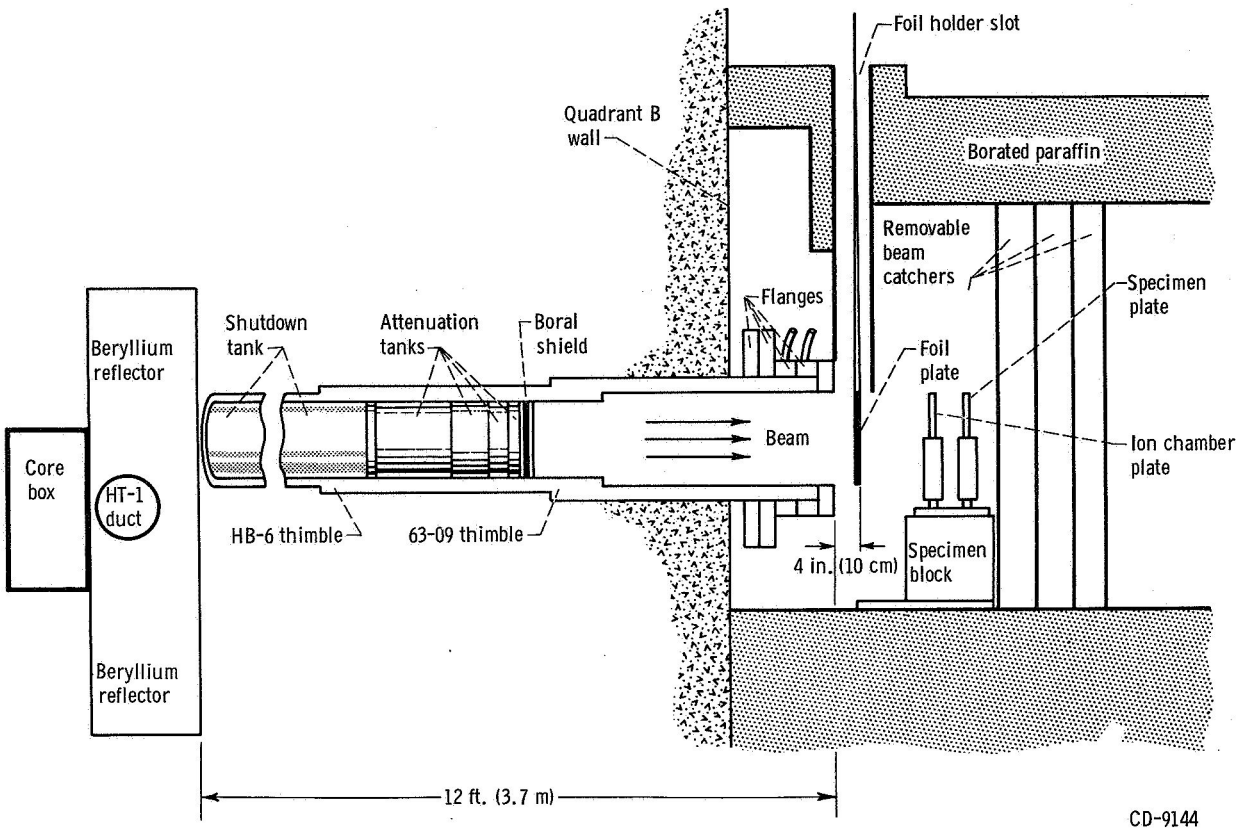

Figure 1. - HB-6 facility.

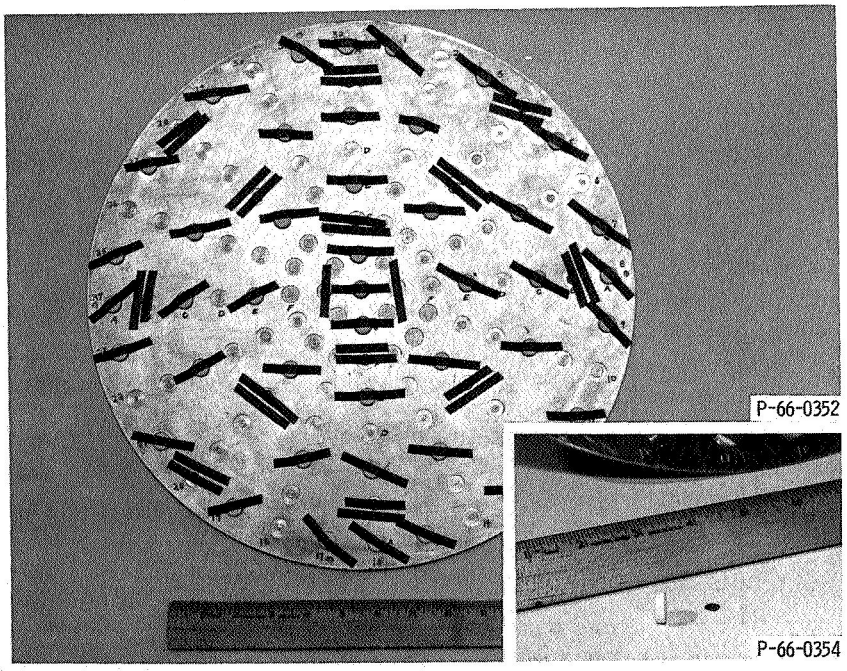

Figure 2. - Typical foil plate with sulfur pellets and gold foils.

M_1 factor compensating for vertical position on foil plate; isoflux (zone) correction factor

M_2 factor compensating for shim-control-rod position

M_3 factor compensating for horizontal position in HB-6 test cavity

M_4 factor compensating for amount of water in attenuation tanks

M_5 factor compensating for reactor power variations

M_6 factor compensating for perturbation in reactor core caused by experiments in other holes (ducts) in reactor

In an attempt to determine and predict the changes in the neutron environment in the HB-6 facility, extensive sulfur pellet and gold-foil activation measurements were performed (ref. 2). The sulfur pellets for fast-neutron determination and the bare and cadmium-covered gold foils for thermal-neutron determinations were taped to the foil plate, as shown in figure 2, and inserted into the HB-6 facility. During each of these

TABLE I. - DATA SAMPLING

(a) Saturated activity for sulfur pellets

Run	Shim-control-rod position		Water thickness		Power, MW	[a]Zone			
						1	2	3	4
	in.	cm	in.	cm		Saturated activity, dis/(sec)(atom)			
3E	19.40	49.3	0	0	60	1.59×10^{-18}	1.52×10^{-18}	1.38×10^{-18}	1.25×10^{-18}
7E	22.54	57.2	0	0	60	1.83	1.74	1.67	1.47
10E	26.84	68.3	0	0	60	1.97	1.92	1.82	1.66
3B	22.91	58.1	6	15.2	60	.023	.0217	.021	.019

(b) Saturated activity for gold film

Run	Shim-control-rod position		Water thickness		Power, MW	Zone		
						1	2	3
	in.	cm	in.	cm		Saturated activity, dis/(sec)(atom)		
3H	18.25	46.4	0	0	60	[b]1.41×10^{-16} [c] .277	[b]1.32×10^{-16} [c] .244	[b]1.16×10^{-16} [c] .219
4H	22.85	58.0	1.5	3.80	60	[b] .73 [c] .112	---------- ----------	---------- ----------
11H	29.20	74.2	0	0	60	[b]1.77 [c] .293	[b]1.67 [c] .28	[b]1.60 [c] .263

[a]Each value for sulfur per zone listed here represents an average of seven or more data points.
[b]Bare gold foil.
[c]Cadmium-covered gold foil corrected for cadmium attenuation.

insertions, one of the six parameters which determine the neutron flux was varied, and the saturated activity associated with each pellet or foil was measured as a function of this parameter. The sulfur-pellet activations were determined by using a 2π beta counter with an efficiency of 0.095 to monitor the phosphorus 32 decay. The gold-foil activations were determined by using a 2π gamma spectrometer. Such a parametric study of the activations yielded specific values for the correction factors M_1 to M_6. A sample of the data obtained from a few insertions is shown in table I. Application of the appropriate activation cross sections (appendixes A and B) to the saturated activities of each foil or pellet resulted in the determination of the standardized fast- and thermal-neutron flux.

ANALYSIS OF SULFUR-PELLET DATA

Determination of Fast-Neutron Correction Factors

Isoflux-zone correction factor M_1. - Each time a foil plate with exposed sulfur pellets was removed from the test cavity and the decay rate determined, isoflux contour lines showing isoflux areas on the test plate were drawn from the data. One such contour map (dashed curves) is shown in figure 3. Analysis of a large number of these contour maps indicates that the foil-plate face can be divided into isoflux zones. Four such

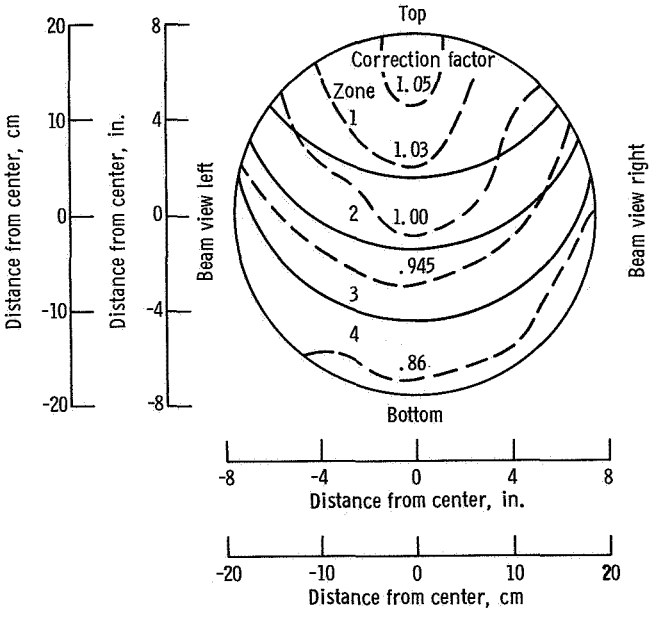

Figure 3. - Isoflux zones for fast neutrons in HB-6 facility as viewed from beryllium reflector.

TABLE II. - FOIL-PLATE ISOFLUX-ZONE CORRECTION FACTORS FOR FAST NEUTRONS

[Error, 4 percent.]

Zone	Correction factor
1	1.056
2	1.000
3	.951
4	.846

zones were chosen, and the average flux (saturated activity) of each zone was compared with that of zone 2, in the center of the foil plate. The solid curves in figure 3 show the position of these zones, and table II gives the values of the normalized correction factors.

Shim-control-rod-position correction factor M_2. - Data similar to those in table I were normalized to zone 2 by using the correction factors of table II and to a reactor power level of 60 megawatts by using the correction factors in figure 4. This procedure resulted in the shim-control-rod-position correction factor M_2. These data corrected for zone and power are compared with the flux (saturated activity) at a shim-control-rod position of 23 inches (58.5 cm). The ratios thus obtained are plotted in figure 5. The smooth curve drawn through the data is the shim-control-rod-position correction factor M_2.

Horizontal-position correction factor M_3. - Sulfur pellets were irradiated on the specimen plate which was 20 inches (50.8 cm) away from the foil plate (fig. 1), to determine whether or not the fast-neutron flux obeyed the inverse-square law within the test cavity of the HB-6 facility. Table III shows the isoflux-zone correction factor obtained at the specimen plate and table IV shows the fractional decrease of the flux from

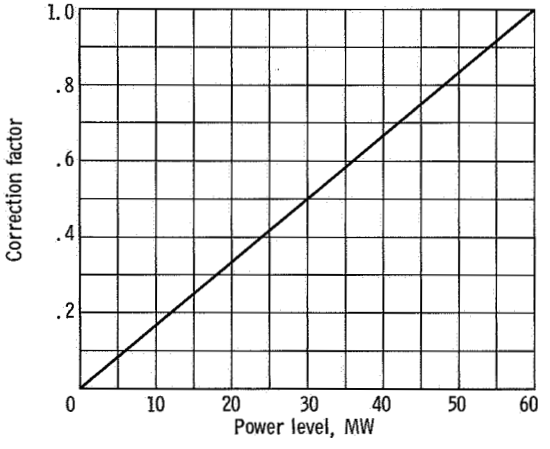

Figure 4. - Reactor power correction factor M_5 for fast and thermal neutrons.

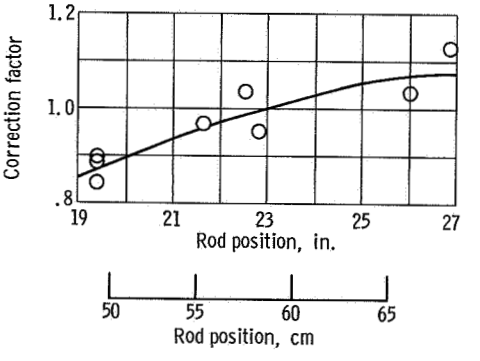

Figure 5. - Shim-control-rod-position correction factor M_2 for fast neutrons.

TABLE III. - SPECIMEN-PLATE ISOFLUX-ZONE CORRECTION FACTORS FOR FAST NEUTRONS

Zone	Correction factors and percentage error
1	1.075±20
2	1.000±10
3	.86±20

TABLE IV. - FRACTIONAL DECREASE OF FLUX FROM VALUES AT FOIL PLATE

Zone	Fractional decrease and percentage error
1	0.72±9.7
2	.71±4.3
3	.72±8.8

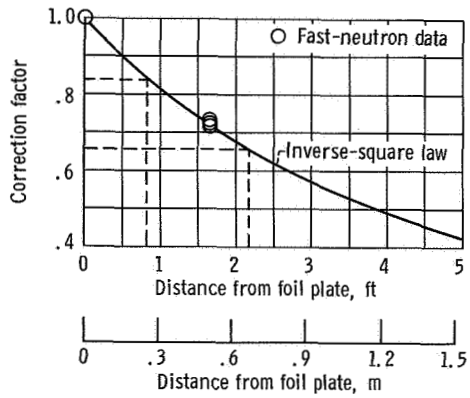

Figure 6. - Horizontal-position correction factor M_3 for fast and thermal neutrons.

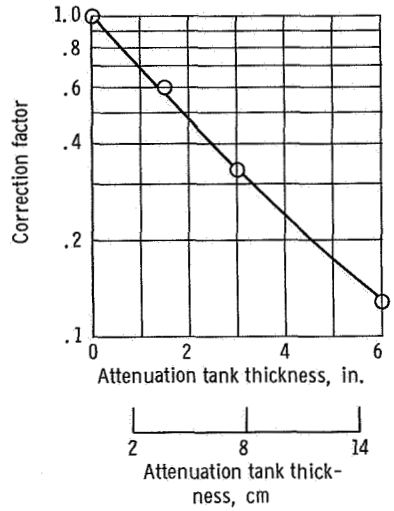

Figure 7. - Water thickness correction factor M_4 for fast neutrons.

values at the foil plate. Within experimental error, the isoflux-zone correction factors are the same for the foil and specimen plate.

The four data points taken from table IV and shown in figure 6 indicate that an inverse-square law can be considered to be the horizontal correction factor. If the specimen-plate position is limited to a distance between 10 and 26 inches (25.4 and 66.0 cm) from the foil plate, the horizontal correction factor is 0.75±0.10. The inverse-square law, as shown in figure 6, permits correction over a wider range.

Attenuation-tank correction factor M_4. - A number of sulfur-pellet activations were performed at various water attenuation test configurations. Data are available for water levels to 6 inches (15.2 cm). Beyond this level the neutron flux is so low that activation measurements are marginal. The results of comparing saturated activities at various water thicknesses to the saturated activity at zero inch of water are shown in figure 7. All data were corrected for power-level and shim-control-rod position by use of figures 4 and 5.

Reactor-power correction factor M_5. - Neutron flux is assumed, on theoretical grounds, to vary in direct proportion to reactor power, as shown in figure 4.

Correction factor due to other experiments M_6. - During the period in which irradiations were being performed in the HB-6 facility, no effect on the test cavity environment was directly traceable to other experiments in the reactor. However, based on calculation (ref. 3), a factor of two increase in the test-cavity neutron levels is possible for the condition of a voided HT-1 duct. This condition is ignored, however, and M_6 is assumed to be 1.

Determination of Standardized Fast Flux

All the actual experimental data were normalized to a shim position of 23 inches (58.5 cm), to zone 2 of the foil plate, to zero inches of water in the water attenuation tanks, and to a reactor power of 60 megawatts by using the correction factors in figures 3 to 7. The data thus normalized yield a standardized saturated activity of 1.69×10^{-18} disintegration per second per atom.

$$A = \int_0^\infty \sigma(E)\varphi(E)\, dE = 1.69\times10^{-18} \text{ dis/(sec)(atom)} \tag{A1}$$

where

$\varphi(E)$ neutron flux as function of energy

$\sigma(E)$ activation cross section for (n, p) reaction in sulfur as function of energy

Using the McElroy (ref. 4) cross section $\overline{\sigma}_M$ of 0.206 barn (0.206×10^{-28} m^2) and threshold energy of 2.48 MeV (0.396 pJ) yields a standardized neutron flux of

$$\varphi_o = \int_{2.48 \text{ MeV}(0.396 \text{ pJ})}^{18 \text{ MeV } (2.88 \text{ pJ})} \varphi(E)\, dE = 8.2\times10^6 \text{ nv} \tag{2}$$

McElroy has quoted ±30 to ±45 percent at a 99.7-percent confidence level in the determination of an averaged cross section $\overline{\sigma}_M$ (ref. 5). In this investigation, an error of ±30 percent was used with the standardized flux φ_o.

ANALYSIS OF GOLD-FOIL DATA

Determination of Thermal-Neutron Correction Factors

Isoflux-zone correction factor M_1. - A large number of gold foils exposed on the foil plate in the test cavity yielded isoflux contour lines, as did sulfur pellets. Isoflux zones (fig. 8) were determined from these isoflux lines in a manner similar to that used with sulfur-pellet data. The correction factors for the zones were obtained by normalizing all zone data to zone 1 of figure 8. The correction factors for isoflux zones for

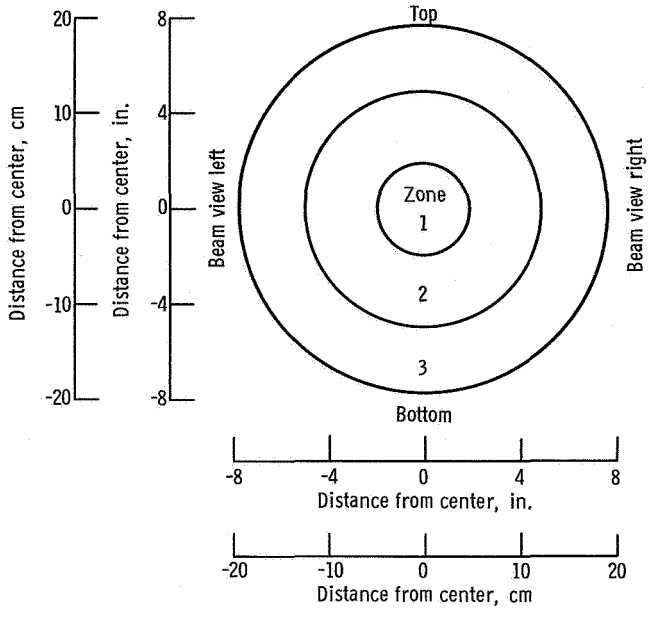

Figure 8. - Isoflux zones for thermal neutrons in HB-6 facility as viewed from beryllium reflector.

TABLE V. - FOIL-PLATE ISOFLUX-ZONE CORRECTION FACTORS FOR THERMAL NEUTRONS

Zone	Correction factor and percentage error
1	1.00±3.2
2	.971±7.2
3	.863±8.8

thermal neutrons are presented in tabular form in table V and in graphic form in figure 8.

Shim-control-rod-position correction factor M_2. - The same procedure was used to determine the thermal flux as a function of shim-control-rod position (fig. 9) as was used in the fast-neutron flux calculations. Figure 9 constitutes the shim-control-rod-position correction factor for thermal neutrons.

Horizontal-position correction factor M_3. - Thermal flux data were not taken at the specimen plate. However, the inverse-square law was applied, and the correction factor shown in figure 6 is used.

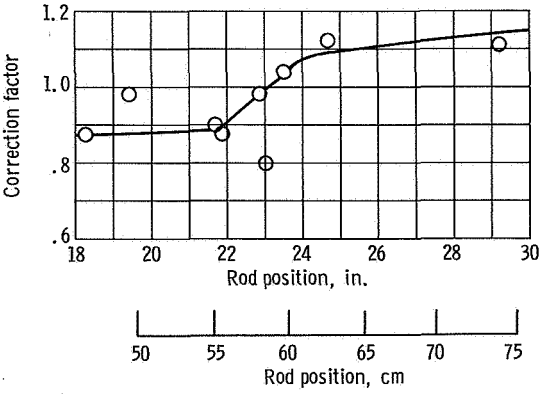

Figure 9. - Shim-control-rod-position correction factor M_2 fo thermal neutrons.

Attenuation-tank correction factor M_4. - Because the thermal flux is small, no consistent data could be correlated with tank condition.

Reactor-power correction factor M_5. - Thermal-neutron flux is assumed, on theoretical grounds, to vary in direct proportion to reactor power in a manner identical to that for fast neutrons, as depicted in figure 4.

Correction factor due to other experiments M_6. - As with the sulfur irradiations, gold-foil irradiations have shown no change in thermal flux that can be directly attributed to perturbations by other experiments in the reactor. Therefore, M_6 is equated to 1.

Determination of Standardized Thermal Flux

From available data, a standardized thermal neutron flux defined in equation (1) can be calculated. All the data were normalized to zone 1 of the foil plate, to a shim-control-rod position of 23 inches (58.5 cm) with no water in the attenuation tanks, and to a reactor power of 60 megawatts by using figures 4 and 8 to 10. Using equation (B5) and letting $\overline{\sigma}$ = 96 barns (9.6×10^{-27} m^2) (ref. 2) yield the standardized thermal flux:

$$\varphi_o = \int_{10^{-8}\ \text{MeV}\ (1.6\times10^{-9}\ \text{pJ})}^{4\times10^{-7}\ \text{MeV}\ (6.4\times10^{-8}\ \text{pJ})} \varphi(E)\ dE = 1.4\times10^{6}\ \text{nv} \qquad (3)$$

Error

A ±30-percent error is inherent in the use of activation foils as a means of determining the absolute fast- and thermal-neutron flux. In this study, to the error associated with the determination of the absolute flux must be added the errors associated with the various correction factors.

Inquiries into the neutron flux of the HB-6 facility necessitate the use of correction factors M_1 to M_6. For these cases, the absolute accuracy of employing equation (1) with these corrections to the fast neutron flux was 35 percent with 90-percent confidence. The thermal-neutron flux error in a similar situation is 38 percent with 90-percent confidence. The errors associated with each correction factor used in equation (1) are listed in table VI, when available.

TABLE VI. - ERRORS ASSOCIATED WITH THERMAL- AND FAST-NEUTRON CORRECTION FACTORS

[Error for standardized flux φ_o, 30 percent; error for reactor power M_5, 10 percent; error for other experiments M_6, 0.]

Neutron	Isoflux zone, M_1	Shim-control-rod position, M_2	Horizontal position, M_3	Attenuation tanks, M_4
	Error, percent			
Fast	4	9.0	12	3.0
Thermal	8.8	20	--	---

EXPERIMENTAL VERIFICATION OF EMPIRICAL FORMULA

Two independent sulfur activations were made to test the accuracy of using equation (1) to predict the fast flux in the test cavity of the HB-6 facility. Equation (1) in one case predicted for a set of reactor and experiment conditions, a flux of 9.1×10^6 neutrons per second per square centimeter (nv) while the measurement yielded 8.8×10^6 neutrons per second per square centimeter (nv). In the second case, for conditions different from the first, equation (1) predicted a flux of 5.0×10^6 neutrons per second per square centimeter (nv) while the sulfur measurement yielded 4.9×10^6 neutrons per second per square centimeter (nv). The actual experimental parameters with the predicted and measured flux are given in table VII. These results strongly suggest that equation (1) can be used to predict the flux in the HB-6 facility within the accuracies specified.

TABLE VII. - INDEPENDENT COMPARISON OF PREDICTED TO MEASURED FAST-NEUTRON FLUX

[Isoflux-zone correction factor, 1; reactor power, 60 MW.]

Rod position		Tanks		Time irradiated, hr	Fast-neutron flux predicted by, nv	Experimental fast-neutron flux, nv	Ratio of experimental flux to predicted flux
		in.	cm				
in.	cm						
27.69	70.4	0	0	6	0.91×10^7	0.88×10^7	0.965
23.69	60.2	1.5	3.8	12	.50	.49	.98

EFFECTS OF NEUTRON SPECTRA

Although a fission spectrum cross section was used to calculate the fast flux from the sulfur-pellet activation data, the actual spectrum may be substantially different from a fission spectrum. The 18-inch- (46-cm) thick slab of beryllium plus a few inches of water that separates the reactor core box from the HB-6 test hole snout could materially change the spectrum of the neutrons as they pass through.

Bloomfield (ref. 6) used the results of a moments calculation of the spectrum through a large thickness of beryllium and calculated the total fast flux (> 0.3 MeV or 0.048 pJ) from sulfur-pellet activation data for this case. This result was 0.75 times that calculated from sulfur activation data using a fission spectrum. The actual spectrum is probably somewhere between the two extremes of the beryllium and fission spectrum. The actual value of the ratio is therefore in the range between 0.75 and 1.00 and could be determined more exactly only by an experimental measurement of the spectrum. The maximum correction is therefore about 25 percent, which is less than the experimental error of 35 percent.

CONCLUSIONS

An empirical prediction equation (eq. (1)) composed of a standardized flux modified by six factors which influence the fast and thermal fluxes was postulated. The six factors which influence the flux take into consideration shim-control-rod position, reactor power, amount of water in the attenuation tanks, horizontal and vertical position in the HB-6 facility, and perturbations in the reactor core caused by other experiments. The standardized flux was experimentally determined at the fiducial test conditions of a reactor power of 60 megawatts, a shim-rod position of 23 inches (58.5 cm), no water in the attenuation tanks, no other experiments in the reactor, and the vertical center point of the foil plate. The standardized fluxes were 8.2×10^6 neutrons per second per square centimeter (nv) ±35 percent for neutron energy exceeding 2.48 MeV (0.396 pJ) and 1.4×10^6 neutrons per second per square centimeter (nv) ±38 percent for thermal neutrons, as measured by sulfur-pellet and gold-foil activation, respectively.

The empirical equation (eq. (1)) successfully predicts flux within the experimental errors. Fast-neutron energy spectrum considerations did not influence the experimental flux determinations beyond the calculated error.

Lewis Research Center,
National Aeronautics and Space Administration,
Cleveland, Ohio, September 11, 1967,
120-27-04-35-22.

APPENDIX A

SULFUR-FOIL ACTIVATION ANALYSIS

The fast-neutron flux in the test cavity of the HB-6 facility was determined using the (n, p) reaction in sulfur. The saturated activity A in disintegrations per second per atom of the resultant phosphorus 32 atom is given by

$$A = \int_0^\infty \sigma(E)\,\varphi(E)\,dE \tag{A1}$$

where $\varphi(E)$ is the neutron flux expressed as a function of energy and $\sigma(E)$ is the activation cross section for the (n, p) reaction in sulfur also expressed as a function of energy (fig. 10). In terms of measurable quantities

$$A = \frac{CR}{\epsilon WM\left(1 - e^{-\lambda t_i}\right)e^{-\lambda t_o}} \tag{A2}$$

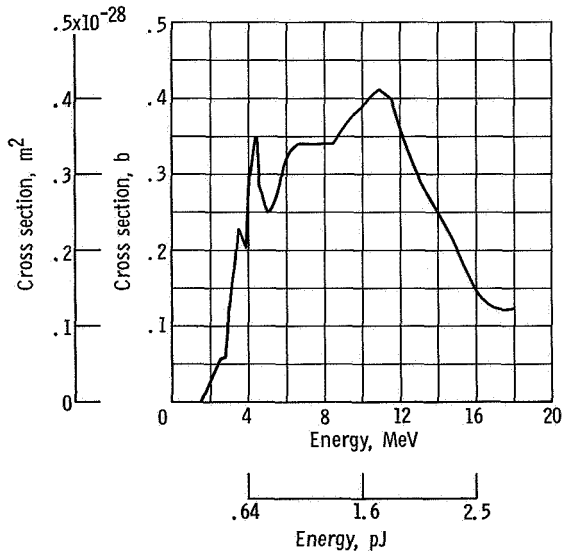

Figure 10. - Activation cross section for sulfur reaction [$S^{32}(n, p)P^{32}$].

where

CR	counting rate of decaying phosphorus 32 atoms
ϵ	efficiency of counter
W	weight of foil sample
M	atoms per unit weight of sample
λ	decay constant of phosphorus 32 atoms
t_i	irradiation time
t_o	decay time

There are at least three methods whereby equations (A1) and (A2) are combined to yield the fast-neutron flux to which the sulfur pellet was exposed. The first method is the Trice method (ref. 7). This method assumes that the energy-dependent cross section for the (n, p) reaction in sulfur can be approximated by a step function. Therefore, equation (A1) can be reduced to

$$A = \overline{\sigma}_T \int_{E_t}^{\infty} \varphi(E)\, dE \tag{A3}$$

The assumption here is that the total activity measured in the sulfur pellet is caused by neutrons whose energy is greater than some threshold energy E_t for which the sulfur pellet has a constant cross section of $\overline{\sigma}_T$. Neutrons with energy less than the threshold energy E_t do not cause sulfur activation because the activation cross section for neutrons whose energy is below E_t is assumed to be zero. The determination of the unknown quantities in equation (A3), namely, $\overline{\sigma}_T$ and E_t, are calculated in the following manner.

An average cross section $\overline{\sigma}_T$ is chosen from the flat part of the curve shown in figure 10. An analytical expression for an energy spectrum of neutrons is also chosen. By the use of a computer and available data on the cross section as a function of energy, the threshold energy E_t is calculated to satisfy equation (A4):

$$\overline{\sigma}_T \int_{E_t}^{18\ \text{MeV}\,(2.88\ \text{pJ})} \eta(E)\, dE \cong \int_{0}^{18\ \text{MeV}\,(2.88\ \text{pJ})} \sigma(E)\eta(E)\, dE \tag{A4}$$

where, for convenience,

$$\int_{18\ \text{MeV}\ (2.88\ \text{pJ})}^{\infty} \eta(E)\ dE \cong 0 \tag{A5}$$

and where

$\bar{\sigma}_T$ average cross section assumed

$\sigma(E)$ actual cross section (fig. 11)

$\eta(E)$ neutron energy spectrum assumed

Under the preceding restraints equation (A3) becomes

$$A = \bar{\sigma}_T \int_{E_t}^{18\ \text{MeV}\ (2.88\ \text{pJ})} \varphi(E)\ dE \tag{A3a}$$

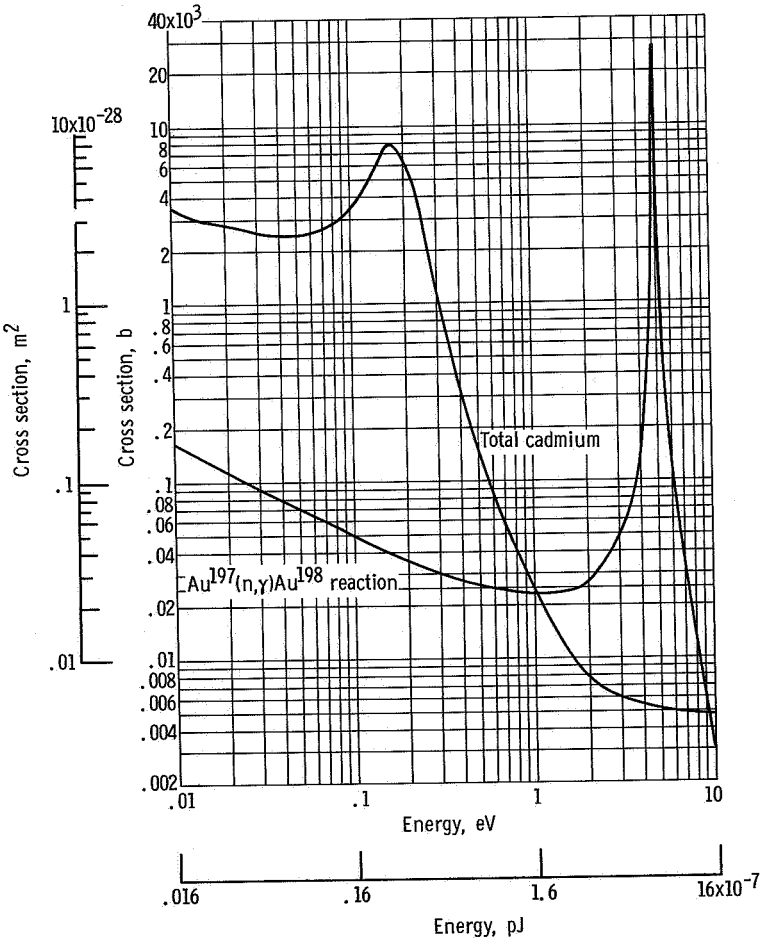

Figure 11. - Cadmium and gold cross sections.

The fast-neutron flux from sulfur activation can also be determined by another method similar to the Trice method. In this method an average cross section is calculated instead of chosen. Again, an energy spectrum for neutrons $\eta(E)$ is assumed, but equation (A4) is modified by not being limited to calculations above a threshold energy E_t. The value of E_t in this method is assumed to be zero. The fission cross section $\bar{\sigma}_f$ is calculated from the following equation:

$$\bar{\sigma}_f = \frac{\int_0^{18\ \text{MeV}\,(2.88\ \text{pJ})} \sigma(E)\eta(E)\ dE}{\int_0^{18\ \text{MeV}\,(2.88\ \text{pJ})} \eta(E)\ dE} \tag{A6}$$

By using the fission cross section to determine neutron flux, equation (A1) now becomes

$$A = \bar{\sigma}_f \int_0^{18\ \text{MeV}\,(2.88\ \text{pJ})} \varphi(E)\ dE \tag{A7}$$

The final method for the determination of the neutron flux from activation data is termed the McElroy method (ref. 4). The actual energy-dependent activation cross section for sulfur (fig. 10) is assumed to be a step function, as in the Trice method. The two unknowns, namely, the average cross section and the threshold energy, must be determined before equation (A1) can be solved for the neutron flux. For this calculation, a neutron energy spectrum $\eta(E)$ is assumed.

Now, equation (A8) is solved for the threshold energy E_t as follows:

$$\int_{E_t}^{18\ \text{MeV}\,(2.88\ \text{pJ})} \sigma(E)\eta(E)\ dE = 0.95 \int_0^{18\ \text{MeV}\,(2.88\ \text{pJ})} \sigma(E)\eta(E)\ dE \tag{A8}$$

or E_t is the energy of neutrons above which 95 percent of the activation takes place.

Here again, for convenience, let

$$\int_{18\ \text{MeV}\,(2.88\ \text{pJ})}^{\infty} \eta(E)\ dE \cong 0 \tag{A9}$$

Once the threshold energy has been calculated, the average cross section $\bar{\sigma}_M$ can be calculated by use of equation (A10):

$$\bar{\sigma}_M = \frac{\int_0^{18\ \text{MeV}\,(2.88\ \text{pJ})} \sigma(E)\eta(E)\ dE}{\int_{E_t}^{18\ \text{MeV}\,(2.88\ \text{pJ})} \eta(E)\ dE} \tag{A10}$$

Now, equation (A1) can be reduced to

$$A = \bar{\sigma}_M \int_{E_t}^{18\ \text{MeV}\,(2.88\ \text{pJ})} \varphi(E)\ dE \tag{A11}$$

In the preceding methods, there is one common drawback. In the calculations of the various threshold energies and average cross sections, the energy spectrum for the neutrons had to be assumed. If this assumed spectrum $\eta(E)$ is different than the spectrum of neutrons $\varphi(E)$ to which the sulfur pellets were actually exposed, the use of equations (A3), (A7), and (A11) will lead to erroneous values for the total flux. In this report, it

TABLE VIII. - EFFECTIVE ENERGIES AND ACTIVATION CROSS SECTIONS FOR SULFUR PELLETS IN VARIOUS NEUTRON ENERGY SPECTRA

Method	Averaged cross section for (n, p) reaction in sulfur pellets, $\bar{\sigma}$		Threshold energy, E_t	
			MeV	pJ
	barns	m^2		
Trice; watt spectrum	0.30	0.30×10^{-28}	2.94	0.470
McElroy; watt spectrum	.206	$.206\times10^{-28}$	2.48	.396
Fission:				
Watt spectrum	.0609	$.0609\times10^{-28}$	0	0
California spectrum	.0597	.0597	0	0
Cranberg spectrum	.0573	.0573	0	0

is assumed that $\eta(E)$ and $\varphi(E)$ are identical Watt fission spectra. The McElroy method was used for the following reasons:

(1) The fission cross-section method, because of its low threshold, is strongly dependent on the neutron energy spectrum. A wrong assumption of a spectrum yields large errors in flux.

(2) Specifying the energy before the average cross section, as in the McElroy method, is a logical approach if the cross section is approximated by a step function.

(3) McElroy's values for the cross section as a function of neutron energy $\sigma(E)$ are more comprehensive than other tabulations. Also his calculation of relations between $\sigma(E)$, E, and $\eta(E)$ are useful.

(4) The arbitrary selection of the average cross section $\bar{\sigma}_T$ in the Trice method leads to an arbitrary solution of equation (A4).

A tabular summary of the various cross-section and threshold energies is given in table VIII (refs. 2 and 4).

APPENDIX B

GOLD-FOIL ACTIVATION ANALYSIS

The thermal-neutron flux in the test cavity of the HB-6 facility was determined by use of the (n, γ) reaction in gold foils. The activation equation (eq. (A1)) applied to gold-foil thermal flux is analyzed in the following paragraphs.

An examination of the $Au^{197}(n, \gamma)Au^{198}$ cross section (ref. 4) in figure 11 shows that equation (A1) can be separated into two component parts, depending on the energy of the neutron causing the activation in the gold foil.

$$A = \int_{10^{-8}\ \text{MeV}\ (1.6\times10^{-9}\ \text{pJ})}^{4.0\times10^{-7}\ \text{MeV}\ (6.4\times10^{-8}\ \text{pJ})} \sigma_{Au}(E)\varphi(E)\ dE + \int_{4.0\times10^{-7}\ \text{MeV}\ (6.4\times10^{-8}\ \text{pJ})}^{18\ \text{MeV}\ (2.88\ \text{pJ})} \sigma_{Au}(E)\varphi(E)\ dE \qquad \text{(B1)}$$

where

A	saturated activity of gold foil
$\sigma_{Au}(E)$	cross section as function of energy for (n, γ) reaction in gold (fig. 11)
$\varphi(E)$	neutron flux energy spectrum

It is assumed that

$$\int_{0}^{10^{-8}\ \text{MeV}\ (1.6\times10^{-9}\ \text{pJ})} \varphi(E)\ dE = 0; \quad \int_{18\ \text{MeV}\ (2.88\ \text{pJ})}^{\infty} \varphi(E)\ dE = 0 \qquad \text{(B2)}$$

The two groups of activities in equation (B1) can be separated experimentally by the cadmium difference method (ref. 2), wherein two gold foils, one cadmium covered and one bare, are irradiated. The activity of the cadmium-covered gold foil is caused primarily by epithermal neutrons ($E > 4.0\times10^{-7}$ MeV or 6.4×10^{-8} pJ), because of the high cross section of cadmium in this region (fig. 11). The bare-gold-foil activity is caused by both the epithermal and thermal neutrons ($E \leq 4.0\times10^{-7}$ MeV or 6.4×10^{-8} pJ).

The saturated activity of a gold foil was obtained by determining the count rate CR of the 0.41-MeV (6.5×10^{-8} pJ) gamma given off by the Au^{198} atom with a sodium iodide thallium (NaI(Tl)) gamma spectrometer and by the application of equation (B3).

$$A = \frac{CR}{\epsilon WM\left(1 - e^{-\lambda t_i}\right)e^{-\lambda t_o}} \tag{B3}$$

where

A	saturated activity of gold foil
CR	counting rate of decaying Au^{198} atoms
ϵ	efficiency of counter
W	weight of gold foil
M	atoms of Au^{197} per unit weight of foil
λ	decay constant of Au^{198} atoms
t_i	irradiation time
t_o	decay time

Before equation (B1) can be used to determine the thermal-neutron flux, three modifications must be made to it because cadmium is used and because gold attenuates the flux. First, cadmium-covered gold foils are not truly impervious to neutrons below an energy of 4.0×10^{-7} MeV (6.4×10^{-8} pJ). Therefore, the fraction f_1 of the total activation of the cadmium-covered gold foil caused by neutrons below 4.0×10^{7} MeV (6.4×10^{-8} pJ) must be calculated. Secondly, the cadmium cover is not completely transparent to neutrons above 4.0×10^{-7} MeV (6.4×10^{-8} pJ). Therefore, the fractional reduc-

TABLE IX. - CADMUIM-COVER AND GOLD-FOIL ATTENUATION CORRECTION FACTORS

Correction factor	Cadmium-cover thickness, mm		
	0.508	1.016	2.032
f_1	.002	0	0
f_2	.016	.030	.058
F_{Cd}	1.42	1.03	1.06
Correction factor	Gold-foil thickness, mm		
	0.128	0.256	0.384
F_{th}	1.075	1.156	1.240

tion f_2 in the activity of cadmium-covered gold foil due to the attenuation of neutrons above 4.0×10^{-7} MeV (6.4×10^{-8} pJ) must be calculated.

Combining these two factors f_1 and f_2 yields a factor F_{Cd} which corrects for the fact that cadmium covers perturb the neutron flux. This factor F_{Cd} when multiplied by the saturated activity of a cadmium-covered foil yields the saturated activity of a cadmium-covered foil without unwanted effects of the cadmium. Thirdly, a gold foil, whether cadmium covered or not, placed in a beam of slow neutrons perturbs the beam and causes a flux attenuation. Therefore, the fraction F_{th} of the activation which thermal neutrons would produce in a gold foil, if it were not for the flux attenuation, must be calculated. All these fractions f_1, f_2, F_{Cd} and F_{th} were calculated for various thickness of cadmium and gold foils and are listed in table IX (ref. 6).

A constant cross section for thermal activation of gold foils is assumed:

$$\int_{10^{-8}\ \text{MeV}\ (1.6\times10^{-9}\ \text{pJ})}^{4.0\times10^{-7}\ \text{MeV}\ (6.4\times10^{-8}\ \text{pJ})} \sigma(E)\varphi(E)\,dE \cong \bar{\sigma}\int_{10^{-8}\ \text{MeV}\ (1.6\times10^{-9}\ \text{pJ})}^{4.0\times10^{-7}\ \text{MeV}\ (6.4\times10^{-8}\ \text{pJ})} \varphi(E)\,dE \tag{B4}$$

By combining equations (B4) and (B1) with the use of the fractions F_{Cd} and F_{th}, the thermal flux ($E < 4.0\times10^{-7}$ MeV or 6.4×10^{-8} pJ) can be calculated from activation analysis of bare and cadmium-covered gold foils by use of the following equations:

$$\Phi_{th} = \frac{F_{th}\left[A^{b}_{Au} - F_{Cd}A^{Cd}_{Au}\right]}{\bar{\sigma}} \tag{B5}$$

where

$$\Phi_{th} = \int_{10^{-8}\ \text{MeV}\ (1.6\times10^{-9}\ \text{pJ})}^{4.0\times10^{-7}\ \text{MeV}\ (6.4\times10^{-8}\ \text{pJ})} \varphi(E)\,dE \tag{B6}$$

and where

Φ	thermal flux
A^{b}_{Au}	measured saturated activity of bare gold foil
A^{Cd}_{Au}	measured saturated activity of cadmium-covered gold foil
$\bar{\sigma}$	averaged cross section for (n, γ) reaction in gold foil (ref. 2)

REFERENCES

1. Smith, John R.; Kroeger, Erich W.; Asadourian, Armen S.; and Spagnuolo, Adolph C.: Fast-Neutron Beam Irradiation Facility in the NASA Plum Brook Test Reactor. NASA TM X-1374, 1967.

2. Dungan, W. E.; and Lewis, J. H.: Nuclear Measurement Techniques for Radiation-Effects Environmental Testing. Rep. No. NARF-62-4T, FZK-9-175, General Dynamics/Fort Worth, Mar. 31, 1962.

3. Bloomfield, Harvey S.: Shielding Requirements for the NASA Plum Brook HB-6 Beamhole Radiation Effects Facility. NASA TM X-1461, 1967.

4. Barrall, R. C.; and McElroy, W. N.: Neutron Flux Spectra Determination by Foil Activation. Volume II: Experimental and Evaluated Cross Section Library of Selected Reactions. (AFWL-TR-65-34, Vol. II, AD-470470), IIT Research Inst., Aug. 1965.

5. McElroy, W. N.; Barrall, R. C ; and Ewing, D.: Neutron Flux Spectra Determination by Foil Activation. Volume I: An Advanced Foil Activation Method of Determining Neutron Flux Spectra for Radiation Effects Studies. (AFWL-TR-65-34, Vol. I, AD-470890), IIT Research Inst., Aug. 1965.

6. Bloomfield, Harvey S.: Calculation of Fast-Neutron Flux Emerging from a Reactor Beamhole and Comparison with Experiment. NASA TM X-1418, 1967.

7. Uthe, Paul M., Jr: Attainment of Neutron Flux - Spectra from Foil Activations. Rep. No. WADC-TR-57-3, Wright-Patterson AFB, Inst. of Tech., Mar. 1957.

NASA-Langley, 1968 — 22 E-3698